Instability of seabed under wave induced loading

Ali Abbasi, Pooya Allahverdizadeh & Behrouz Gatmiri
Department of civil engineering- University of Tehran, Tehran, Tehran, Iran

2011 Pan-Am CGS Geotechnical Conference

ABSTRACT
In this study, several models are presented for analysis of sea floor movement produced by storm waves. They are based on the finite element method, and used to predict dimension of stress and strain in seabed sediment subjected to wave pressure loading. These models based on elastic and elasto-plastic behavior, and they simplify in two-dimensional modeling. Large deformation of soil skeleton occurs below the mud line. The analysis of these models with both linear and nonlinear soils properties are generated for typical offshore soils. The results indicate that under relatively huge surface wave, high stress and deformation will be occurred. This deformation can distribute to considerable depths of seabed sediment. These soil's deformations can induce large lateral force on offshore pile and pipeline.

RÉSUMÉ
Plusieurs modèles sont présentés pour l'analyse du mouvement au sol de la mer produite par les vagues de tempête. Ils se sont basés sur la méthode des éléments finis, et sont utilisés pour supputer la dimension de contrainte et de déformation dans les sédiments du fonds de marins soumis à une charge d'onde de pression. Ces modèles se sont basés sur le traitement élastique et élasto-plastique et ils sont simplifiés par la modélisation à deux dimensions. les grandes déformations du squelette du sol se sont produites au-dessous de boue. ces modèles analyse à la fois les propriétés des sols linéaires et non linéaires sont générés pour les sols typiques off-shore. Les propriétés employées dans ces modèles sont sélectionnées parmi des sols typiques des off-shore. Le traitement de ces sols est analysé à deux manières, linéaire et non-linéaire. Les résultats indiquent sous la charge de grande vagues sont constatées de très grand contrainte et déformations. Ces déformation peuvent développer au profondeur considérable. elles peuvent aussi causer de grands forces latérales sur pieux off-shore et de pipelines.

1 INTRODUCTION

Seabed instability owing to gravity, wave, or earthquake forces may result in massive submarine slide. This phenomena is one of the important factors affecting the safety of the facilities, such as pipelines, oil storage tanks, oil production platforms in ocean areas.

When wave is formed, it produced a pressure pattern extending down to the porous seabed with change in stresses. Customarily, the instability induced in the seabed by the wave has been researched by either total stress or effective stress concepts. In both analyses, the wave-induced water pressure on the seabed surface is considered as an external force. The physical meaning of this external force, however, is different for these two approaches. In the total stress approach, the wave-induced water pressure is treated as surface force acting on the seabed surface, whereas in the effective stress analysis, it is converted to the seepage force which is a body force acting on the soil skeleton. One of the possible reason for such z difference is attributed to the drainage condition in the seabed. In the case of an impermeable seabed consisting of clay or mud, total stress analysis can be applied (Henkel, 1970). In order to investigate effective stress analysis is preferable because it is closely related to the deformation and failure of the soil skeleton.

There are two solutions for calculating the seabed response, the analytical and the numerical solution. In this field, both the solutions are in elastic manner of soil skeleton. Two different mechanisms occur for wave-induce instability, namely, Shear failure and liquefaction.

In this paper, both analytical and numerical solution in elastic manner compare with numerical solution based on elasto-plastic behavior of the soil. Instability of the soil which occurred in this modeling is related to shear failure mechanism.

2 THEORETICAL BACKGROUND

Limiting the analysis to the flow, pore pressures and effective stresses induced in a porous bed by plane, periodic waves propagating in water of essentially constant depth *d,* it suffices to consider the two-dimensional problem illustrated in Fig.1

As the governing equation for flow of a compressible pore fluid in a compressible porous medium the generally accepted form of the consolidation equation (Biot, 1941) or storage equation (Verruit, 1969) is adopted. For two-dimensional problem and treating the porous bed as hydraulically anisotropic with principal permeability K_x *and* K_z in x and z-direction, respectively, this equation may be written in the form

$$\frac{k_x}{k_z}\frac{\partial^2 p}{\partial x^2}+\frac{\partial^2 p}{\partial z^2}-\frac{\gamma_w n\beta}{k_z}\frac{\partial^2 p}{\partial t}=\frac{\gamma_w}{k_z}\frac{\partial \varepsilon}{\partial t} \qquad [1]$$

$$\beta=\frac{1}{k'}=\frac{1}{k_w}+\frac{1-S_r}{p_{w0}} \qquad [2]$$

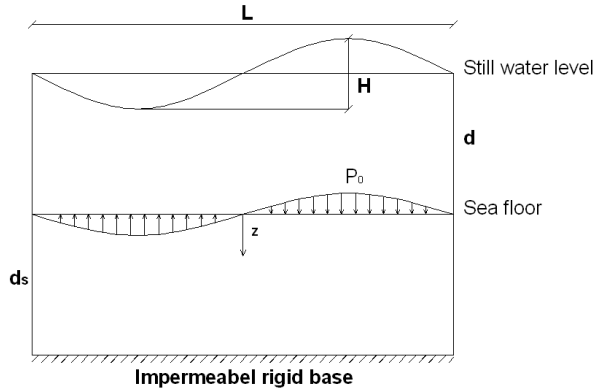

Figure 1. Definition of Wave-seabed interaction problem.

The equation of equilibrium which relate soil displacements, volume strain and pore pressure, are given by

$$G\nabla^2 u + \frac{G}{(1-2\mu)}\frac{\partial \varepsilon}{\partial x} = \frac{\partial p}{\partial x} \quad [3]$$

$$G\nabla^2 v + \frac{G}{(1-2\mu)}\frac{\partial \varepsilon}{\partial z} = \frac{\partial p}{\partial z} \quad [4]$$

$$\varepsilon = \frac{\partial u}{\partial x} + \frac{\partial v}{\partial z} \quad [5]$$

In equation (1)-(5), p is the wave-induced pore pressure, γ_w is the unit weight of the pore-water, n is soil porosity, β is compressibility of the pore fluid, t is time, ε is the volume strain, K_w is true bulk modulus of elasticity of water, P_{w0} is the absolute pore-water pressure, S_r is degree of saturation, and G is shear modulus.

For linear waves propagating over the sea floor a harmonic pressure positive under the crest and negative under the trough is induced on the mud line; the hydrodynamic pressure can be given as shown by

$$p(x,t) = p_0 \exp\left[i\left(\lambda x - \omega t\right)\right] \quad [6]$$

where $p_0=(\gamma_w H)/(2\mathrm{Cosh}(\lambda d))$. Considering a soil deposit infinitely deep limited by a horizontal surface, the wave-induced effective stresses, displacements and pore pressures for most of the soil can be written as (Yamamoto, 1978, Madsen, 1978)

$$\frac{\sigma_x'}{p_0} = \frac{\sigma_z'}{p_0} = -i\frac{\tau_{xz}}{p_0} = \lambda z \exp(-\lambda z)\exp\left[i\left(\lambda x - \omega t\right)\right] \quad [7]$$

$$\frac{2\lambda G u}{p_0} = -i\,\lambda z\,\exp(-\lambda z)\exp\left[i\left(\lambda x - \omega t\right)\right] \quad [8]$$

$$\frac{2\lambda G v}{p_0} = (1+\lambda z)\exp(-\lambda z)\exp\left[i\left(\lambda x - \omega t\right)\right] \quad [9]$$

$$\frac{p}{p_0} = \exp(-\lambda z)\exp\left[i\left(\lambda x - \omega t\right)\right] \quad [10]$$

3 PRINCIPAL STRESSES

The wave-induced shear stress at a point within the sediment may become large to overcome its shearing resistance, causing it to fail. The actual mode of such instability will depend on the spatial distribution of wave-induced shear failure and the shear strength of the sediments. Conventionally, prediction of failure for soils has been based on Mohr-Coulomb's failure criterion, which remains the most widely used in geotechnical engineering. Although other criteria of failure have been suggested in the literature (Griffiths, 1986, 1990), the Mohr-Coulomb's failure criterion is used here because of its simplicity and conservation. Principal stresses only the wave-induced incremental changes in effective stresses and pore pressure within soils from the initial equilibrium have been considered. Thus, the effective normal stresses $\tilde{\sigma}_x'$, $\tilde{\sigma}_y'$ and $\tilde{\sigma}_z'$ in x, y and z directions are given by:

$$\tilde{\sigma}_x' = \tilde{\sigma}_{x0}' - \tilde{\sigma}_x' = -(\gamma_z - \gamma_\omega)K_0 z - \sigma_x' \quad [11]$$

$$\tilde{\sigma}_y' = \tilde{\sigma}_{y0}' - \tilde{\sigma}_y' = -(\gamma_z - \gamma_\omega)K_0 z - \sigma_y' \quad [12]$$

and

$$\tilde{\sigma}_z' = \tilde{\sigma}_{z0}' - \tilde{\sigma}_z' = -(\gamma_z - \gamma_\omega)K_0 z - \sigma_z' \quad [13]$$

where $\tilde{\sigma}_{x0}'$, $\tilde{\sigma}_{y0}'$ and $\tilde{\sigma}_{z0}'$ in x, y and z directions, respectively, while γ_w and γ_s are the unit weights of water and soil, respectively. In Equations [11]-[13], K_0 is the coefficient of earth pressure at rest and is related to the poisson's ratio μ as

$$K_0 = \frac{\mu}{1-\mu} \quad [14]$$

Since the shear stresses on the horizontal and vertical planes are zero at the initial equilibrium, the effective shear stresses $\Pi\tau_{xz}'$, $\Pi\tau_{yz}'$ and $\Pi\tau_{xy}'$, are given as

$$\tilde{\tau}_{xz}' = -\tau_{xz}' \quad [15]$$

$$\tilde{\tau}_{yz}' = -\tau_{yz}' \quad [16]$$

$$\tilde{\tau}_{xy}' = -\tau_{xy}' \quad [17]$$

For study of the general stresses fields that occur in a complicated boundary value problem, it is convenient use principal stress space. The principal stress space also leads to a convenient geometric representation of various failure criteria. The effective principal stresses $\tilde{\sigma}_1'$, $\tilde{\sigma}_2'$ and $\tilde{\sigma}_3'$ can be expressed as (Griffiths, 1986)

$$\tilde{\sigma}_1^{'} = \frac{\tilde{S}}{\sqrt{3}} + \sqrt{\frac{2}{3}}\,\tilde{t}\,\mathrm{Sin}\left(\alpha - \frac{2\pi}{3}\right) \quad [18]$$

$$\tilde{\sigma}_2^{'} = \frac{\tilde{S}}{\sqrt{3}} + \sqrt{\frac{2}{3}}\,\tilde{t}\,\mathrm{Sin}\left(\alpha\right) \quad [19]$$

$$\tilde{\sigma}_3^{'} = \frac{\tilde{S}}{\sqrt{3}} + \sqrt{\frac{2}{3}}\,\tilde{t}\,\mathrm{Sin}\left(\alpha + \frac{2\pi}{3}\right) \quad [20]$$

Where

$$\tilde{s} = \frac{1}{\sqrt{3}}\left(\tilde{\sigma}_x^{'} + \tilde{\sigma}_y^{'} + \tilde{\sigma}_z^{'}\right) \quad [21]$$

$$\tilde{t} = \sqrt{\frac{\left(\tilde{\sigma}_x^{'} - \tilde{\sigma}_y^{'}\right)^2 + \left(\tilde{\sigma}_y^{'} - \tilde{\sigma}_z^{'}\right)^2 + \left(\tilde{\sigma}_z^{'} - \tilde{\sigma}_x^{'}\right)^2 + 6\left(\tau_{xy}^{'\,2} + \tau_{yz}^{'\,2} + \tau_{zx}^{'\,2}\right)}{3}} \quad [22]$$

$$\alpha = \frac{1}{3}Sin^{-1}\left(\frac{-3\sqrt{6J_3}}{\tilde{t}^3}\right) \quad [23]$$

in which

$$J_3 = S_x S_y S_z - S_x \tilde{\tau}_{yz}^{'} - S_y \tilde{\tau}_{xz}^{'} - S_z \tilde{\tau}_{xy}^{'} + 2\tilde{\tau}_{yz}^{'}\tilde{\tau}_{xz}^{'}\tilde{\tau}_{xy}^{'} \quad [24]$$

$$S_x = \tilde{\sigma}_x^{'} - \frac{\tilde{s}}{\sqrt{3}} \quad [25]$$

$$S_y = \tilde{\sigma}_y^{'} - \frac{\tilde{s}}{\sqrt{3}} \quad [26]$$

$$S_z = \tilde{\sigma}_z^{'} - \frac{\tilde{s}}{\sqrt{3}} \quad [27]$$

Equation [18]-[20] ensure that $\tilde{\sigma}_1' \le \tilde{\sigma}_2' \le \tilde{\sigma}_3'$.

4 MOHR-COULOMB MODEL IN ABAQUS

The Mohr-Coulomb failure or strength criterion has been widely used for geotechnical applications. Indeed, a large number of the routine design calculations in the geotechnical area are still performed using the Mohr-Coulomb criterion.

The Mohr-Coulomb criterion assumes that failure is controlled by the maximum shear stress and at this failure shear stress depends on the normal stress. This can be represented by plotting Mohr's circle for states of stress at failure in terms of the maximum and minimum principal stresses. The Mohr-Coulomb failure line is the best straight line that touches these Mohr's circles. Thus, the Mohr-Coulomb criterion can be written as

$$\tau = C - \sigma \tan\varphi \quad [28]$$

where τ is the shear stress, σ is the normal stress (negative in compression), C is the cohesion of the material, and φ is the material angle of friction. The Mohr-Coulomb criterion written above in terms of the maximum and minimum principal stresses can be written for general states of stress in terms of three stress invariants. These invariants are the equivalent pressure stress as

$$p = \frac{1}{3}trace\left(\boldsymbol{\sigma}\right) \quad [29]$$

where $\boldsymbol{\sigma}$ is the principle effective stress matrix and the Mises equivalent stress as

$$q = \sqrt{\frac{3}{2}\left(\boldsymbol{S} : \boldsymbol{S}\right)} \quad [30]$$

where **S** is the effective stress deviator matrix, defined as

$$\boldsymbol{S} = \boldsymbol{\sigma} + p\boldsymbol{I} \quad [31]$$

and the third invariant of deviatoric stress is

$$r = \left(\frac{9}{2}\boldsymbol{S} : \boldsymbol{S} : \boldsymbol{S}\right)^{\frac{1}{3}} \quad [32]$$

The Mohr-Coulomb yield surface is then written as

$$F = R_{mc}q - p\,\tan\phi - C \quad [33]$$

where ∅ is the friction angle of the material in the meridional stress plane, C represents the evolution of the cohesion of the material in the form of isotropic hardening

(or softening) and $R_{mc}$is the Mohr-Coulomb deviatoric stress measure defined as

$$R_{mc}\left(\Theta,\phi\right)=\frac{1}{\sqrt{3}Cos\,\phi}Sin\left(\Theta+\frac{\pi}{3}\right)+\frac{1}{3}Cos\left(\Theta+\frac{\pi}{3}\right)\tan\phi \quad [34]$$

where Θ is the deviatoric polar angle defined as

$$Cos\left(3\Theta\right)=\left(\frac{r}{q}\right)^3 \quad [35]$$

in the Mohr-Coulomb Potential flow is assumed, so

$$d\,\varepsilon^{pl}=\frac{d\,\tilde{\varepsilon}^{pl}}{g}\frac{\partial G}{\partial\sigma} \quad [36]$$

Where $d\varepsilon^{pl}$ is the differential of plastic strain, $d\tilde{\varepsilon}^{pl}$ is the differential of equivalent plastic strain, ***g*** can be written as

$$g=\frac{1}{C}\boldsymbol{\sigma}:\frac{\partial \boldsymbol{G}}{\partial\sigma} \quad [37]$$

and G is the flow potential, chosen as a hyperbolic function in the meridional stress plane and a smooth elliptic function in the deviatoric stress plane:

$$G=\sqrt{\left(\in C\big|_0\tan\psi\right)^2+\left(R_{mw}\,q\right)^2}-p\tan\psi \quad [38]$$

where ψ is the dilation angle measured in the $p-R_{mw}$ plane at high confining pressure, $c|_0$ is the initial cohesion yield stress, and ϵ is a parameter, referred to as the eccentricity, that defines the rate at which the function approaches the asymptote (the flow potential tends to a straight line as the eccentricity tends to zero). This flow potential, which is continuous and smooth in the meridional stress plane, ensures that the flow direction is defined uniquely in this plane. The function asymptotically approaches a linear flow potential at high confining pressure stress and intersects the hydrostatic pressure axis at 90°.

The flow potential is also continuous and smooth in the deviatoric stress plane (the Π-plane); we adopt the deviatoric elliptic function used by Menétrey and Willam (1995):

$$R_{mw}\left(\Theta,e\right)=\frac{4\left(1-e^2\right)Cos^2\left(\Theta\right)+\left(2e-1\right)^2}{2\left(1-e^2\right)Cos\,\Theta+\left(2e-1\right)\sqrt{4\left(1-e^2\right)Cos^2\Theta+5e^2-4e}}\times R_{mc}\left(\frac{\pi}{3},\phi\right) \quad [39]$$

Where e is a parameter that describes the "out-of-roundedness" of the deviatoric section in terms of the ratio between the shear stress along the extension meridian ($\Theta=0$) and the shear stress along the compression meridian ($\Theta=\frac{\pi}{3}$). The out-of-roundedness parameter, e, is dependent on the friction angle φ; it is calculated by matching the flow potential to the yield surface in both triaxial tension and compression in the deviatoric plane:

$$e=\frac{3-Sin\varphi}{3+Sin\varphi} \quad [40]$$

Flow in the meridional stress plane can be close to associated when the angle of friction, ϕ, and the angle of dilation, ψ, are equal and the eccentricity parameter, ϵ, is very small; however, flow in this plane is, in general, nonassociated. Flow in the deviatoric stress plane is always nonassociated. Therefore, the use of this Mohr-Coulomb model generally requires the solution of nonsymmetric equations.

According the yamamoto formulation, If we want observe only the effect of the wave pressure on soil without gravity load effect, the wave induced stress in plane strain condition is

$$\frac{\tilde{\sigma}'}{p_0}=\begin{pmatrix}\lambda z\exp\left(-\lambda z\right)Cos\left(\lambda x-\omega t\right) & \lambda z\exp\left(-\lambda z\right)Sin\left(\lambda x-\omega t\right)\\ \lambda z\exp\left(-\lambda z\right)Sin\left(\lambda x-\omega t\right) & -\lambda z\exp\left(-\lambda z\right)Cos\left(\lambda x-\omega t\right)\end{pmatrix} \quad [41]$$

in one length of the wave, the principle stress is

$$\frac{\tilde{\sigma}'}{p_0}=\begin{pmatrix}\lambda z\exp\left(-\lambda z\right) & 0\\ 0 & -\lambda z\exp\left(-\lambda z\right)\end{pmatrix} \quad [42]$$

in this situation, the maximum effective stress is

$$\frac{\tilde{\sigma}'_{\max}}{p_0}=\lambda z\exp\left(-\lambda z\right)=\frac{C\times Cos\varphi}{p_0} \quad [43]$$

From [43] we can calculate the depth in which soil become plastic.

5 2D FINITE ELEMENT MODEL

According to table 1, four models with two different elastic properties and two permeabilities were assumed. The soil in these models is isotropic and homogenous

The wave characteristic is showed in table 2.the value of maximum wave induced pore pressure is similar to some report from Gulf of Mexico. The boundary condition was shown in Figure 1. The amplitude of harmonic pressures on the seabed surface becomes P_0 =70 kN/m^2. The pressure with time increase than 10000s and after this time the pressure is constant. Lateral boundaries have zero pore pressure in all time.

Table1. Properties of soil and dimensions of models.

Characteristics	Model 1	Model 2	Model 3	Model 4
Permeability(m/s)	1E-3	1E-6	1E-3	1E-6
Elastic module(N/m^2)	2.7E6	2.7E6	2.7E7	2.7E7
μ, Poisson's ratio	0.3	0.3	0.3	0.3
n, Porosity	0.6	0.6	0.6	0.6
S_r, Saturation	100%	100%	100%	100%
φ, internal friction angle	30°	30°	30°	30°
Delation angle	0°	0°	0°	0°
C_0 (N/m^2)	2.5E4	2.5E4	2.5E4	2.5E4
Depth(m)	200	200	200	200
Length(m)	200	200	200	200

Table 2. Characteristics of Wave.

Characteristics of wave	All Models
d; Water depth(m)	30
T; Wave period(s)	13.2
H; Wave height(m)	20.7
L; Wave length(m)	200
P_0(N/m^2)	7E5

The seabed was divided into 400 Quadratic element with rough rigid and impermeable base (u=0, v=0), lateral boundaries is fixe in z direction (v=0), in Mud line, $\sigma_z = P$, u and v is free.

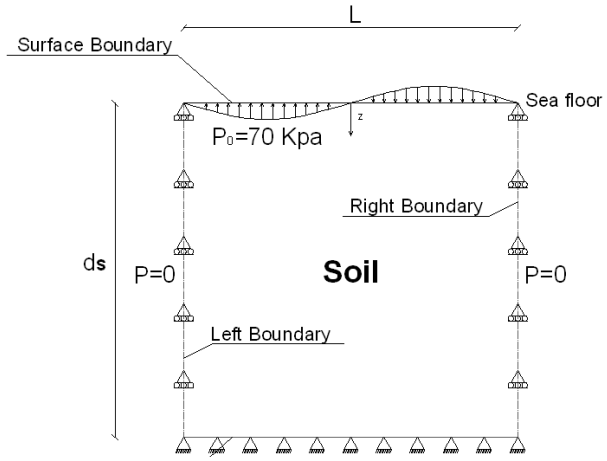

Figure 2. Boundary condition (Displacement and pore pressure)

6 EFFECT OF PERMEABILITY AND ELASTICITY

Soil analysis was used in ABAQUS model. The total time is 1E5 s and one factor multiple to pore pressure which is top of the soil boundary condition. This factor change from 0 to 1 as time change from 0 to 1E4 s. according to Equation [43] maximum effective stress is 21650 kN/m^2 and the depths of the model that become plastic is 16.6 m and 54.5 m below the mud line. In FE model minimum depth is 10 m and maximum is 55 m.

Because we apply the pore pressure slightly at time 8407s in 32m below the mud line, the soil become plastic and after this, the layer of soil become plastic which the thickness of this layer achieve to 40 m.

Fig 3. shows the layer of soil which became plastic.

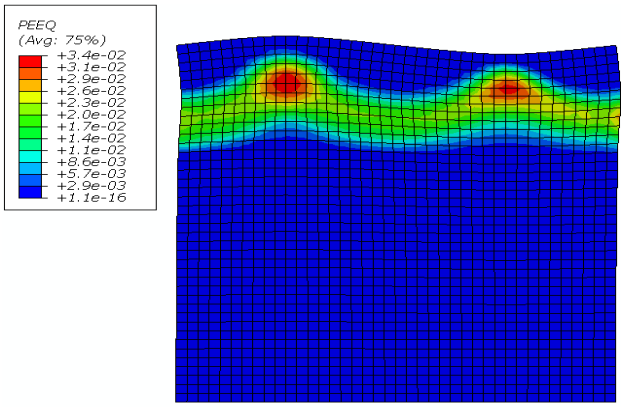

Figure 3. Equivalent plastic strain on model 1.

Maximum depth of plastic deformation is 55m below the mud line and minimum depth is 10m below the mud line (t=1E5 s). The maximum displacements of models in 32 m below the mud line, the depth of the maximum effective

stress is shown in Table 3. In all models soil at time 8407 s became plastic.

Table 3. Maximum horizontal displacement at 30m below mud line

Characteristics	u_{max}(m)	Total Run time(s)
Model 1	0.4361	8900
Model 2	0.7914	1E5
Model 3	0.0458	9023
Model 4	0.0641	9783

In comparing models with variation of permeability, the effect of permeability on elastic and final plastic deformation is negligible. But at same time equal 8900 s in all models the ratio of plastic deformation under elastic deformation for K=1E-6 m/s in both module elasticity is 1.16 and this ratio for K=1E-3 is 1.22.

Figure 4 to 6 shows stress profiles at maximum effective stress $\tilde{\sigma}'_x$, $\tilde{\sigma}'_z$, $\tilde{\sigma}'_{xz}$. About 30 m to 55 m below the mud line the stresses approximately are constant and equal with 21650 kN/m2.

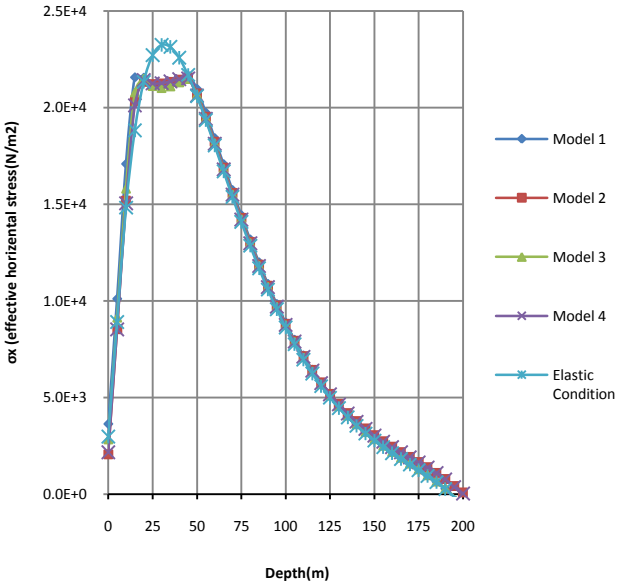

Figure 4. Effective horizontal stresses in plastic and elastic condition in same time (t=8900s).

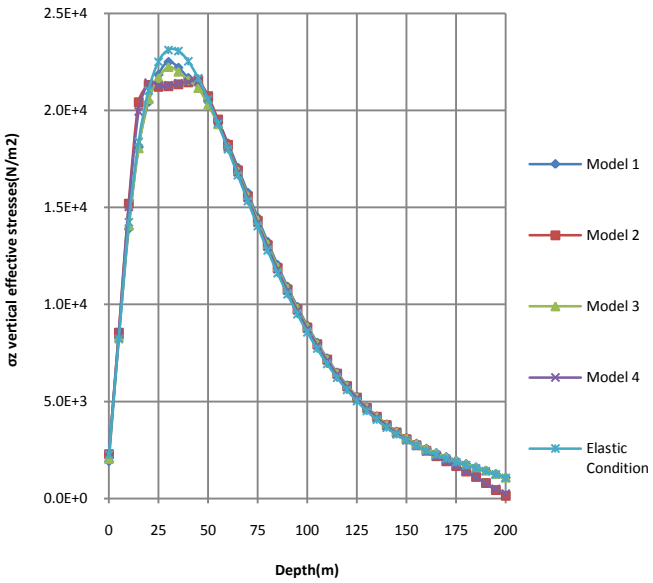

Figure 5. Effective vertical stresses in plastic and elastic condition in same time (t=8900s).

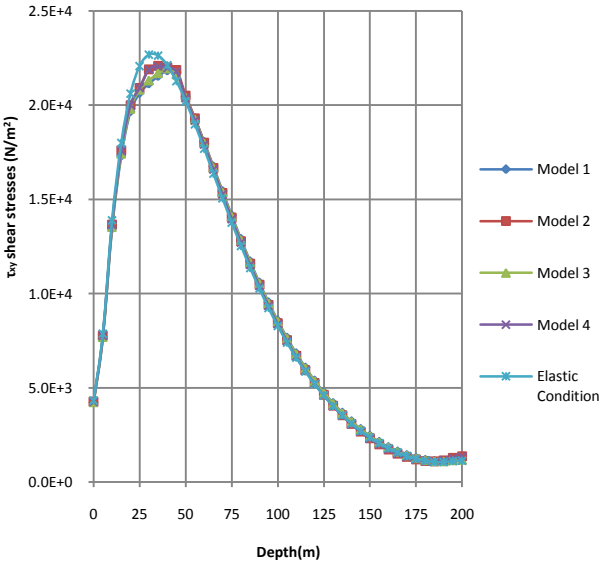

Figure 6. Effective shear stresses in plastic and elastic condition in same time (t=8900s).

Figure 7 show displacement in x and z direction (u, v) at maximum displacement. from 30m to 55m below mud line the soil become plastic. At depth 55 m, gradient of diagram changed. This point is the bound between plastic zone and elastic zone.

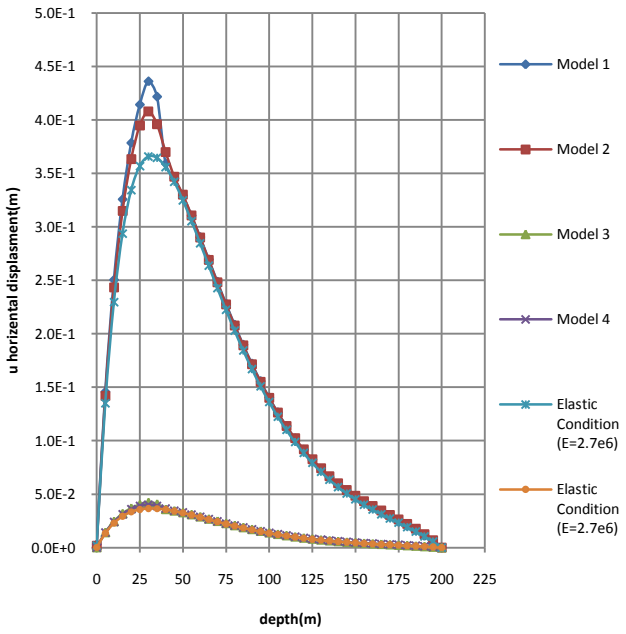

Figure 7. Horizontal displacements in plastic and elastic conditions in same time (t=8900s).

7 CONCLUSION

The result in plastic condition show that in depth 30m and 55m below the mud line and by attention to module of elasticity, the displacement until 3 time increase according to total time of analysis. The total time of analysis is a function of total time of storm. Because of convergence of analysis, the loading of model is gently whereas in fact, this behavior acts rapidly.

The plastic zone in all models with any module of elasticity and any permeability is in layer with extreme thickness of 38 m. this depth is only in relation with C_0 and φ. This zone actually is the place which instability occurs on it.

The effect of permeability on final displacement is negligible, and the ratio of plastic deformation in same time is increase whenever the permeability increases.

In fact, Value of final displacement depends on modulus of elastic but starting of plastic displacement is depends on wave characteristic and soil characteristic. According to the result of analysis, displacement continues until model became non convergent. This manner shows that soil is unstable.

In this paper, Models is only under wave load but actually, soil in sea bed is sloping and gravity load act to become it unstable. However weight of soil causes to increase the normal stress and increase the value of maximum shear straight, but the component of gravity load with slope direction decreases the shear straight of soil. The models have not any slope but the result of analyzing can help to find the unstable slop at a definite wave.

8 REFRENCES

ABAQUS, 2009. Abaqus Theory Manual 6.9.1, *ABAQUS*, Inc.

Biot, M.A. 1941. General theory of three-dimensional consolidation, *Journal of Applied Physics*, 12: 155-164.

Gatmiri, B. 1990, A Simplified Finite Element Analysis of Wave-Induced Effective Stresses and Pore Pressures in Permeable Sea Bed, *Géotechnique*, 40 No. 1: 15-30.

Griffiths, D. V. 1986. Some Theoretical Observations on Conical Failure Criteria in Principal Stress Space, *International Journal of Solids and Structures*, 22: 553-565.

Griffiths, D. V. 1990. Failure Criteria Interpretation based on Mohr-Coulomb Friction, *Journal of Geotechnical Engineering*, ASCE. 116, 986-999.

Henkel, D.H. 1970. The role of Waves in causing submarine landslides, *Geotechnique*, 20 (1): 75-80.

Jeng, D.S. 1997. Wave-Induced Seabed Instability In Front of A Breakwater, *Ocean Engineering*, 24:887.

Jeng, D.S., Cheng L. 2000. Wave-Induced Seabed Instability Around a Buried Pipeline In a Poro-Elastic Seabed, *Ocean Engineering*, 27:127.

Jeng, D.S. 2001, Mechanism of The Wave-Instability Seabed Instability In Vicinity of a Breakwater: a Review, *Ocean Engineering*, 28:537.

Madsen, O. S. 1978. Wave-induced Pore Pressures and Effective Stresses in a Porous Bed, *Géotechnique*, Vol. 28, No. 4, 377-393.

Menétrey, P.H. and Willam K. J. 1995. Triaxial Failure Criterion for Concrete and its Generalization, *ACI Structural Journal*, 92: 311–318.

Verruijt, A. 1969. Elastic Storage of Aquifers in Flow Through Porous Media, Chapter 8, De Wiest, R. J. M. (ed.). Academic Press, 31-376.

Wright, S.G., Dunham, R. 1972. Bottom Stability under Wave Induced Loading, Proc. *4th Annual Offshore Technology Conferences*, paper 1603 1, Houston, Texas, 853-862.

Yamamoto, T. 1978. Seabed Instability from Waves, *10th Annual Offshore Technology Conferences*, paper 3262 1, Houston, Texas, 1819-1824.